Science World Journal Vol. 19(No 2) 2024 https://dx.doi.org/10.4314/swj.v19i2.15
www.scienceworldjournal.org
ISSN: 1597-6343 (Online), ISSN: 2756-391X (Print)
Published by Faculty of Science, Kaduna State University

Full Length Research Article

EXTRACTION OF REDUCING SUGARS FROM BIOMASS AND CONVERSION TO BIOACTIVE FATTY ACID ESTERS USING [CU-BDC@SiO_2] AS CATALYST AND ITS DOCKING STUDIES

Amamat Yakubu Asimu, Samaila Muazu Batagarawa, Nura Suleiman Gwaram*, Muhammad Saleh Salga, Abubakar Sani, Aminu Musa

Department of Pure and Industrial Chemistry, Umaru Musa Yar'adua University, P.M.B. 2211, Katsina State, Nigeria

*Corresponding Author Email Address: nura.suleiman@umyu.edu.ng

ABSTRACT
This research investigates the extraction of biomass-derived reducing sugars from sugarcane bagasse and their dehydration to fatty acids. The fatty acids were esterified to bioactive fatty acid esters using a catalyst. The contents of the active extracts were analyzed by spectroscopic methods (FT-IR, TGA, ED-XRF, and GC-MS). Applying *in silico* molecular modeling study, the compounds' possible bioactivity was examined. The compounds were explored for their hepatoprotective potential against selected targets: TNFα (PDB ID: 6MKB), TNF receptor (PDB ID: 1XU2), and GSH reductase (PDB ID: 2LV3). From the results of the docking analysis, compound A was identified to have a binding energy of -6.4 kcal/mol, -5.4 kcal/mol, and -4.8 kcal/mol against the target proteins respectively. Assessed for their drug-likeness and bioavailability, all compounds were found to follow the Lipinski rule of five, Ghose, Veber, Egan, and Muegge criteria. None of the molecules violated more than one of Lipinski's rules of five. In this regard, the compounds showed good drug-likeness and pharmacokinetic scores, suggesting their potential to be highly bioavailable and active oral drugs with low toxicity. Based on the results, it can be concluded that the bioactive compounds can be used as hepatoprotective agents.

Keywords: Sugarcane Bagasse; Fatty acid esters; *In Silico* Molecular docking; Hepatoprotective activity.

INTRODUCTION

Utilizing natural crops is a solution to several environmental problems, including global warming, air and water pollution, and contamination. Currently, lignocellulosic biomass is extensively utilized in the production of several high-value products because of its year-round feasibility, low cost, and plentiful availability. Crop processing generates enormous amounts of waste, which are traditionally burned or disposed of carelessly, polluting the environment (Awoyale *et al.,* 2021). Ethnobotany is being used in modern drug research to search for pharmacologically active components (phytochemicals) in plants so as to alleviate the severe side effects of synthetic drugs (Hassan *et al.,* 2022).These phytochemicals are known to perform various functions and have been established to possess myriad biological activities ranging from antibacterial, antifungal, antiviral, antioxidant, anticancer, hepatoprotective, antitumor benefits, and so much more. Sugarcane (*Saccharum oficinarum* Linn.) is a well-known crop of the family Poaceae. The demand for sugarcane-derived products is increasing worldwide; its production increased from 1.7 to 1.9 billion tonnes from 2008 to 2018. Many farmers in Nigeria's northern part of West Africa depend on sugarcane cultivation as their means of livelihood. These sugarcanes are sold to people in towns, marketplaces, villages, and other regions of the nation, in addition to sugar refineries. After being chewed or refined, the bagasse from these canes usually gets thrown away as garbage, littering the environment. Through this study, this "waste" was channeled into a useful purpose due to its availability and low cost (Ezeonuegbu *et al.,* 2021).

A vital organ that is important for the body's elimination of xenobiotics is the liver. Liver diseases pose a serious threat to public health and the pharmaceutical sector as well as medical personnel. Botanical drugs are commonly used in the treatment of liver problems because the standard approach is linked with several adverse effects (Meharie et al., 2020). Lipid peroxidation and other forms of oxidative damage are the main ways whereby most hepatotoxic chemicals damage liver cells (Adewusi and Afolayan, 2010).

In this study, the extraction of biomass-derived reducing sugars from sugarcane bagasse, followed by dehydration of extracted sugars to fatty acids and its subsequent esterification to bioactive fatty acid esters using 1,4-benzenedicarboxylic acid, metal and silica [Cu-BDC][SiO_2] as heterogeneous catalyst. The potential application of the fatty acid esters on hepatoprotective activity using molecular docking was investigated.

MATERIALS AND METHODS

Reagents and instrumentation

All chemicals were of analytical grades and used without any further purification. Hydrochloric acid, Sulphuric acid, Phosphoric acid, and Ethanol were purchased from Aldrich–Sigma Company. Dimethylformamide (DMF) was purchased from Kernel Ltd. Hydrogen Peroxide and Sodium hydroxide was purchased from Central Drug House. Copper nitrate from Nice Chemicals Pvt., Ltd and 1,4 - benzene dicarboxylic acid from Loba Chemie Pvt., Ltd. Silica and Glucose were obtained from Park Scientific Limited. pH was determined using a pH meter instrument. FTIR spectra were determined with an Agilent Technologies FTIR Spectrophotometer. Elemental Composition was carried out using an EDXRF Analyzer. TGA, GC-MS

Collection and Preparation of sample

Sugarcane bagasse (SCB) was collected from several sugarcane vendors at the Central Market of Katsina State, Nigeria. The bagasse was soaked and washed with distilled water; air dried for 48 h and crushed to a particle size of 0.1 to 0.2 mm, then screened using a sieve with a pore size of 1 mm. The crushed SCB was transferred into polythene bags, sealed, and stored for later use. To have access to the reducing sugars, pretreatment was done to remove hemicellulose and lignin.

Science World Journal Vol. 19(No 2) 2024 https://dx.doi.org/10.4314/swj.v19i2.15
www.scienceworldjournal.org
ISSN: 1597-6343 (Online), ISSN: 2756-391X (Print)
Published by Faculty of Science, Kaduna State University

Sugarcane bagasse pretreatment
The acid and alkaline pretreatment was carried out in two steps, according to the method of Guilherme *et al.* (2017) with some modifications.

Acid pretreatment
This first step of pretreatment was carried out using 20 g of bagasse immersed in a 2 % sulfuric acid solution in a 200 mL flask. The mixture was subjected to heating at 121 °C for 30 min, and then the resulting solid fraction washed with what distilled water until pH 7.0 and then filtered with Whatmann filter paper and used in the second step.

Alkali pretreatment
This second step of pretreatment was carried out using the acid-treated bagasse immersed in 2 % sodium hydroxide solution in a 200 mL flask. The mixture was subjected to heating at 121 °C for 30 min. After this, the pH of the mixture was adjusted to 7.0 using hydrochloric acid. The pretreated bagasse was washed with distilled water, filtered with Whatman filter paper, and stored at 4 °C before use.

Acid Hydrolysis of Sugarcane bagasse to reducing sugar
Hydrolysis was carried out using 10 mL of 1 % H_2SO_4 added to the solids in a 200 mL conical flask and the mixture was heated to 120 °C for 40 min using an autoclave. After hydrolysis, the product was centrifuged at 200 rpm for 20 min to separate the solid and liquid samples. The liquid of the pretreated sample was then filtered using filter paper to separate the solid residue. After that, liquid–liquid extraction was carried out for the separation of sugars from the aqueous phase using 20 mL ethyl acetate in a separating funnel. The organic layer was analyzed by FTIR. (Method adopted by Ariffin *et al.* (2020) with modifications.

Dehydration of extracted sugars to fatty acid.
100 mL of sugar solution (hydrolysate) was added to 5 mL phosphoric acid and heated to 150 °C using a heating mantle for 90 minutes. After the treatment, the solution was cooled down to room temperature and vacuum-filtered using a Whatmann filter paper. The filtrate was separated using liquid–liquid extraction to separate the organic phase from the aqueous phase using 20 mL ethyl acetate in a separating funnel. The organic layer was analyzed by FTIR (Jung *et al.,* 2021) with modifications.

Fourier-transform infrared spectroscopy (FTIR) analysis: An FTIR spectrum of reducing sugars and fatty acids was done using a Vertex 70/70V Spectrophotometer (Agilent Technologies) for identification of major functional groups.

Preparation of [Cu-BDC][SiO_2] catalyst
In a mechanochemical preparation process, 2 mmol hydrated copper nitrate (0.4832 g), and 1 mmol (0.06008 g) of silica (SiO_2) was added to a mortal. Then, 150 mg (0.15 g) of 1, 4- benzene dicarboxylic acid was added followed by adding 0.5 mL of the solvent (DMF) while grinding continuously, and the mixture was gently ground to get a homogenous mixture. After that, the mixture was monitored for possible reactivity for 8h to obtain [Cu-BDC][SiO_2]. After these, the desired products would be isolated by centrifugation, the catalyst then washed with ethanol for three or more times and dried in a vacuum oven at 70 °C overnight (Guo *et al*., 2019 with modifications).

Characterization of the Cu-BDC and [M-BDC][SiO_2] catalyst
Fourier-transform infrared spectroscopy (FTIR) analysis: An FTIR spectrum of the synthesized catalyst was done using Vertex 70/70V Spectrophotometer (Agilent Technologies) for identification of possible vibration frequencies functional groups. The FT-IR spectrometer was scanned over the frequency range of 650-4000 cm^{-1} at a resolution of 16 cm^{-1}.

X-ray fluorescence (**XRF) analysis:** The synthesized catalyst was analyzed by ED-XRF (energy dispersive X-ray fluorescence) to obtain the elemental composition of the catalysts.

Thermogravimetric analysis: The synthesized catalyst was analyzed for the determination of high thermal stability and weight loss by thermogravimetry (TGA).

Catalytic Test
The catalytic esterification of fatty acids with alcohol over terephthalic acid was carried out in a 250 mL round-bottom flask equipped with a condenser, thermocouple, and magnetic stirrer. The flask was loaded with sugars (20 mL), alcohol (20 mL), and catalyst (0.10 g). The solution was heated to the reflux temperature of the respective alkyl alcohol at a constant stirring speed of 500 rpm for a period of 9 h. The reflux temperature of ethanol was 78.4 °C. After the reaction was completed, the mixture was cooled to room temperature, and the product was isolated i.e. separated by centrifugation and diluted with anhydrous ethanol, the supernatant was characterized by GC-MS (Guo *et al*., 2019) with modifications.

Identification of compounds by Gas chromatography-mass spectrometry (GC-MS) analysis
Compounds from esterification reaction were identified by gas chromatography-mass spectrometry GC-MS (Agilent 19091S-433UI GC/MSD) using an HP-5MS Ultra Inert column (30m × 250 µm I.D., × 0.25 µm film thickness), analyzed over a mass per charge (*m/z*) range of 50–500 and identified by comparing the mass spectra with the NIST (National Institute of Standards and Technology) mass spectral library. NIST MS Search 2.3 was used for mass spectra comparison (NIST Mass Spectrometry Data Center, 2017). The GC-MS was equipped with a splitless injector. The temperature of the injector was 300 °C. The oven condition was 100 °C for 3min, which was increased by 10 °Cmin^{-1} to 300 °C held for 7 min followed by 5 °Cmin^{-1} ramping to 325 °C and held for 1 min. Helium was used as the carrier gas (15mL/min).

Molecular docking Analysis
The Toshiba Satellite Pro was used and Windows 8 as the primary operating system, ChemDraw Ultra 12.0 for structure, Chem 3D Pro 12.0 for conversion and energy minimization, AutoDock vina in PyRx-virtual screening tools for docking process, and Discovery Studio Visualizer 2020 (v19.1.0.18287) for visualization and observation of docking result were used. preADMET and SwissADME free web tools for ADMET and drug-likeness predictions were used.

Structure generation
The structure of the ester compounds was drawn using Chem Draw Ultra 12.0 and converted from 2D to 3D structures using Chem 3D Pro 12.0 and saved in the MOL format.

Energy minimization
Energy minimization was carried out to reduce constraints in the structures before finding the most stable geometry of the studied molecules. The converted 3D structures were minimized using MM2 (Merck Molecular mechanics) and then saved in pdb format using Chem 3D Pro 12.0 integral option (save as/Protein Data Bank). The ligand molecules were then loaded in AutoDock tools in PyRx for further ligand preparation process. Non-polar hydrogens were merged and rotatable bonds were also determined and adjusted. The prepared ligand was then saved in AutoDock pdbqt format (Sengupta *et al.,* 2021).

Ligand preparation
The structures of four natural products from the extract are named 6-Acetyl-.beta.-d-mannose, 9-Octadecenoic acid (Z)-,2-hydroxy-1-(hydroxymethyl) ethyl ester, 9-Octadecenoic acid (Z)-,2,3-dihydroxy propyl ester, and Z-4-Nonadecen-1-ol acetate were assigned alphabetically as A, B, C, and D respectively. The ligand files were prepared using PyRx Software Tools 1.5.7 (the Scripps Research Institute, La Jolla, CA, USA) and finally written in pdbqt file format for docking analysis.

Protein preparation
The 3D structures of protein targets named TNFR (PDB ID: 1XU2), GSH reductase (PDB ID: 2LV3), and TNF*α* (PDB ID: 6MKB) were retrieved from the RCSB Protein Data Bank and saved in pdb format. PDB contains a large number of proteins which are experimentally determined and stored in this site. These files were introduced to BIOVIA Discovery Studio Visualizer 4.5 software to remove water molecules, and add polar hydrogen atoms, removing chains or heteroatom not required, and computing charges (kollman charges). Finally, the protein files were written in pdbqt file format for docking analysis (Muhammad *et al.,* 2020).

***In Silico* molecular docking**
Docking analysis was performed by using AutoDock Vina software integrated into the PyRx-virtual screening tool (Scripps). The ligands were docked into the target structures and the interactions of the docked complexes were studied visually with the help of Discovery Studio Biovia 2020. The results were displayed in terms of binding affinity and analyzed the protein–ligand interactions (Sengupta *et al.,* 2021).

Protein-ligand complex visualization: The protein-ligand complexes were visualized using the Discovery Studio 2020 software. Using this software, the polar and hydrophobic interactions between ligand and target were characterized, and 2D and 3D illustrations of such interactions were generated (Taghizadeh *et al.,* 2022).

Pharmacokinetic studies of the compounds by ADMET analysis
The ADMET properties of the compounds were assessed using pre-ADMET platform version 2.0. The assessment was carried out for each physiochemical property (Absorption, Distribution, Metabolism, Excretion, and Toxicity) by submitting an SMILE format of the individual compound obtained from Chem Draw. The corresponding basic information and experimental values of these entries form the basis for prediction on a new compound established on computational similarity check (Muhammad *et al.,* 2020).

ADME and Drug likeness analysis
To determine the drug-likeness properties of the selected compounds, the pre-ADMET and SwissADME platform 2017 was used (Daina and Zoete, 2016). Three-dimensional structures of the compounds from Chem 3D Pro 12.0.2 were submitted through the platform. The compounds were screened for drug-likeness properties based on several expert criteria that are used in drug design considered crucial for any drug candidate. The most commonly used rules considered in this work include; Lipinski's rule, Ghose's rule, Egan's rule, Veber's rule, and Muegge's rule (Muhammad *et al.,* 2020).

Boiled-EGG analysis
For predicting blood-brain barrier (BBB) permeability, gastrointestinal absorption (GI), P-glycoprotein- (Pgp-) mediated efflux, and the capacity to be used as substrates of cytochrome P450 (CYP), Boiled-EGG was used. The BOILED-EGG plot analysis was analyzed using the Swiss ADME web server, a free web tool available at http://www.swissadme.ch/ (Sengupta *et al.,* 2021).

RESULTS AND DISCUSSION

Hydrolysis of SCB analysis result
Reducing sugars were extracted from agricultural wastes (SCB) using an acid and alkaline hydrolysis process.

Science World Journal Vol. 19(No 2) 2024 https://dx.doi.org/10.4314/swj.v19i2.15
www.scienceworldjournal.org
ISSN: 1597-6343 (Online), ISSN: 2756-391X (Print)
Published by Faculty of Science, Kaduna State University

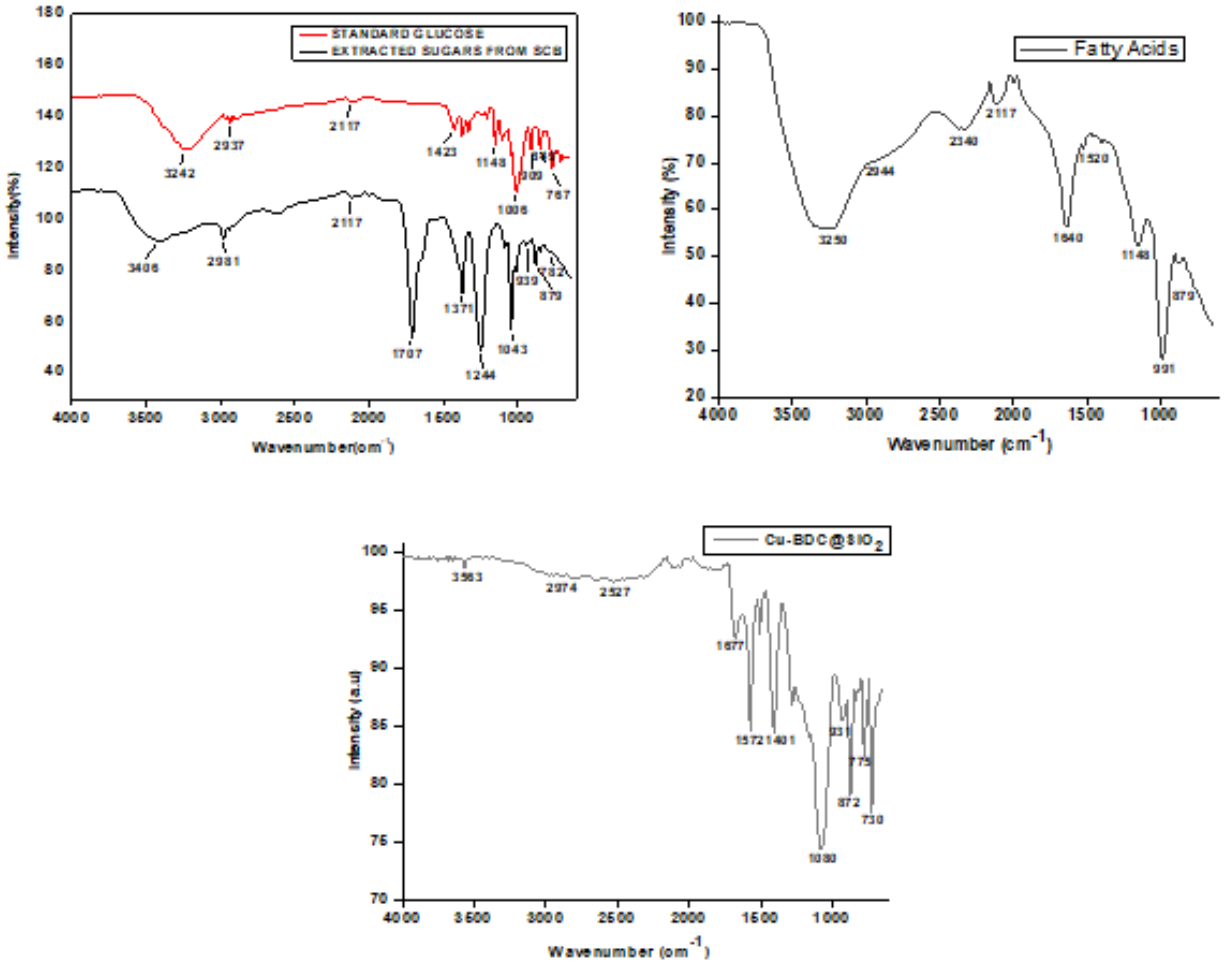

Figure 1: FTIR spectra for catalyst (Cu-BDC@SiO_2), reducing sugars extracted from SCB and produced fatty acids

FT-IR is an effective analytical technique to confirm the existence of functional groups and Figure 1 shows the FT-IR spectra of the prepared [Cu-BDC@SiO_2] metal-organic framework, reducing sugars extracted from SCB and produced fatty acids. The peaks in the spectral range of 3400-3600 may be due to crystalline water or acidic O-H of the carboxylic group or ethanol. The observed peaks at 1565 and 1684 cm^{-1} are attributed to the symmetric stretching of -C=C- and carboxylate group C=O groups of H_2BDC (where H_2BDC is benzene dicarboxylic acid). The peaks at 872 cm^{-1} and 775 cm^{-1} are attributed to (C-H) bending vibrations of aromatic rings in the linker molecule. So the existence of an aromatic ring shows that the organic ligand (linker) is present in the final product. The absorption band at 1080 cm^{-1} can be attributed to the Si-O-Si stretching vibration. A peak at 2974 cm^{-1} attributed to the aliphatic (C-H) asymmetric stretching vibration of DMF. The appearance of an important band at 730 cm^{-1} relates to the stretching vibration of Cu-O showing that the MOF structures with Cu and BDC molecules remained stable during silica coating, which is in good agreement with data reported by Bagheri *et al.,* 2020 and Salama *et al.,* 2018.

Science World Journal Vol. 19(No 2) 2024 https://dx.doi.org/10.4314/swj.v19i2.15
www.scienceworldjournal.org
ISSN: 1597-6343 (Online), ISSN: 2756-391X (Print)
Published by Faculty of Science, Kaduna State University

Energy-dispersive X-ray fluorescence analysis

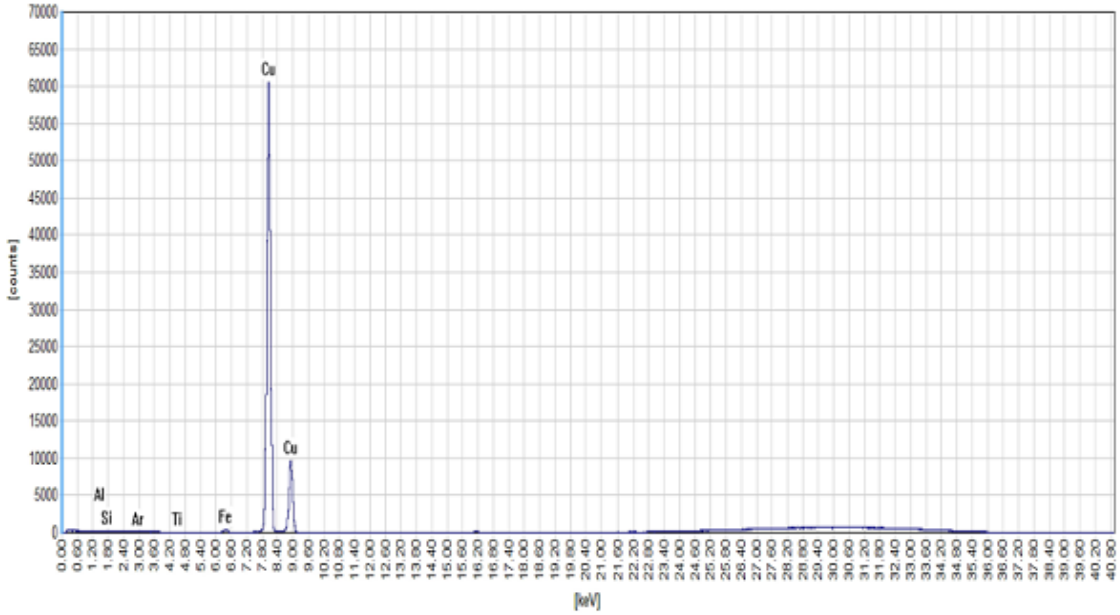

Figure 2: EDXRF result of the synthesized catalyst (Cu-BDC@SiO_2).

EDXRF analysis of the prepared catalyst Cu-BDC@SiO_2 was analyzed for carbon from the linker BDC, copper from the metal, and silica from SiO_2. The result confirmed the presence of carbon, copper, and silica in the prepared catalyst and provided the elemental composition ratio as shown in Figure 2

Thermogravimetric analysis TGA

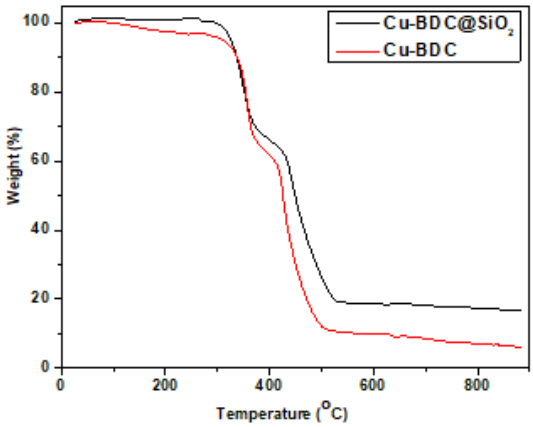

Figure 3: TGA analysis of the synthesized catalyst Cu-BDC and Cu-BDC@SiO_2

The thermal stability of Cu-BDC was investigated by thermogravimetric analysis (TGA) under a N_2 atmosphere. As illustrated in Figure 3, it is evident that the thermal characteristics of both catalysts are almost alike. The thermogram can be described in successive stages. The first weight loss (3 %) for all samples in the region between 50 and 110 °C resulted from the loss of physically adsorbed water molecules, the region between 110~300 °C with a weight loss of 27 % was observed due to the liberation of the DMF solvent that is physically adsorbed in internal pores. However, Cu-BDC@ SiO_2 lost about 30 % of its weight. The weight loss in the temperature range of 300~370 °C was determined to be 12 % for Cu-BDC and 10 % for Cu-BDC@SiO_2, the structure started to lose the chemically bonded water, which needs a higher temperature than the physically adsorbed water to be released, while the loss of 46 % in the temperature range of 370~440 °C corresponds to decomposition of the BDC-ligand of Cu-BDC and 40% for Cu-BDC@ SiO_2. The results of the TGA indicate that all samples presented excellent thermal stability before 370 °C. No weight loss beyond 500 was observed in figure 3. These findings are in agreement with those reported for Cu-BTC MOF which has similar catalytic properties (Peedikakkal *et al*., 2020).

Esterification reaction analysis

An oily residue (milky-colored) was obtained after the esterification of fatty acids with ethanol as a reagent and solvent to prepare long-chain alkyl ethyl esters. During the experiments carried out to prepare fatty acid alkyl esters an additional transesterification reaction was observed under the conditions used during the reaction treatment by a continuous liquid-liquid extraction resulting from the reaction mixtures mixed with ethyl acetate; under these conditions, generated a transesterification that in situ converted FAs to FAEEs, this initial synthesis of FAEEs by transesterification, ethyl acetate was used as the mutual solvent for solubilizing sugar and free fatty acid similar to the method used by Chaparro and Urbina, in 2022.

Gas Chromatography-Mass Spectroscopy Analysis

This method is suitable for the analysis of compounds that are volatile as such or after derivatization (Inarkar and Lele, 2012). Clarification of the type and composition of esters formed were characterized using Gas Chromatography-Mass Spectrometry (GC-MS). The identification through GC-MS analysis carried out revealed the composition of fatty acid components and ethyl esters

Science World Journal Vol. 19(No 2) 2024 https://dx.doi.org/10.4314/swj.v19i2.15
www.scienceworldjournal.org
ISSN: 1597-6343 (Online), ISSN: 2756-391X (Print)
Published by Faculty of Science, Kaduna State University

formed in the reaction. In this study, 4 different compounds were identified by GC-MS analysis of fatty acids and esters ranging from C_8-C_{21}. Components were identified from the database Library of GC-MS instrument (NIST14.L). Identified compounds with their name, molecular formulas, retention time, and peak percentages are illustrated in table 1. These compounds were used in this study for molecular docking analysis.

Table 1: GC-MS profile of compounds identified from esterification reaction of fatty acids

S. No	Name of Compound	Molecular Formula	Molecular Weight	RT	Peak Area %
1	6-Acetyl-.beta.-d-mannose	$C_8H_{14}O_7$	222.19	14.111	0.19
2	9-Octadecenoic acid (Z)-, 2-hydroxy-1 (hydroxymethyl)ethyl ester	$C_{21}H_{40}O_4$	356.54	23.035	38.32
3	9-Octadecenoic acid (Z)-,2,3-dihydroxy propyl ester	$C_{21}H_{40}O_4$	356.54	26.239	33.81
4	Z-4-Nonadecen-1-ol acetate	$C_{21}H_{40}O_2$	324.54	29.500	27.67

Molecular Docking Result Analysis

Table 2: The binding energies between the docked compounds with the prospective proteins

Target Protein	Ligand	Binding energy(kcal/mol)
TNF*α* receptor (PDB ID: 1XU2)+	6-Acetyl-.beta.-d-mannose	-6.4
	9-Octadecenoic acid(Z)-,2-hydroxy-1-(hydroxymethyl) ethyl ester	-5.3
	9-Octadecenoic acid (Z)-,2,3-dihydroxy propyl ester	-5.2
	Z-4-Nonadecen-1-ol acetate	-4.7
GSH reductase (PDB ID: 2LV3)+	6-Acetyl-.beta.-d-mannose	-4.8
	9-Octadecenoic acid(Z)-,2-hydroxy-1-(hydroxymethyl) ethyl ester	-4.5
	9-Octadecenoic acid (Z)-,2,3-dihydroxy propyl ester	-4.7
	Z-4-Nonadecen-1-ol acetate	-4.3
TNF*α* (PDB ID: 6MKB)+	6-Acetyl-.beta.-d-mannose	-5.3
	9-Octadecenoic acid(Z)-,2-hydroxy-1-(hydroxymethyl) ethyl ester	-5.4
	9-Octadecenoic acid (Z)-,2,3-dihydroxy propyl ester	-5.2
	Z-4-Nonadecen-1-ol acetate	-5.3

The Gibbs free energy (kcal/mol) suggests an equilibrium state and complex stability in the protein-ligand binding process (Taghizadeh *et al*., 2022). From the docking study, the best binding affinities of the four compounds based on binding are listed in table 2 above. The binding pose for each ligand molecule was analyzed and the lowest ligand energy with these proteins among different poses was generated. The lower energy scores represent the best protein-ligand target binding affinity compared to higher energy scores ranging from -4.3 to -6.4 kcal/mol.

From table 2, 6-Acetyl-.beta.-d-mannose compound-A, -Octadecenoic acid(Z)-,2-hydroxy-1-(hydroxymethyl) ethyl compound B and 6-Acetyl-.beta.-d-mannose compound A was identified to have the lowest binding energy of -6.4 kcal/mol, -5.4 kcal/mol, and -4.8 kcal/mol among the compounds investigated for target protein TNFR (PDB ID: 1XU2), TNF*α* (PDB ID: 6MKB) and GSH reductase (PDB ID: 2LV3). Respectively

Science World Journal Vol. 19(No 2) 2024 https://dx.doi.org/10.4314/swj.v19i2.15
www.scienceworldjournal.org
ISSN: 1597-6343 (Online), ISSN: 2756-391X (Print)
Published by Faculty of Science, Kaduna State University

Structural proteins of hepatoprotective (Interactive analysis)

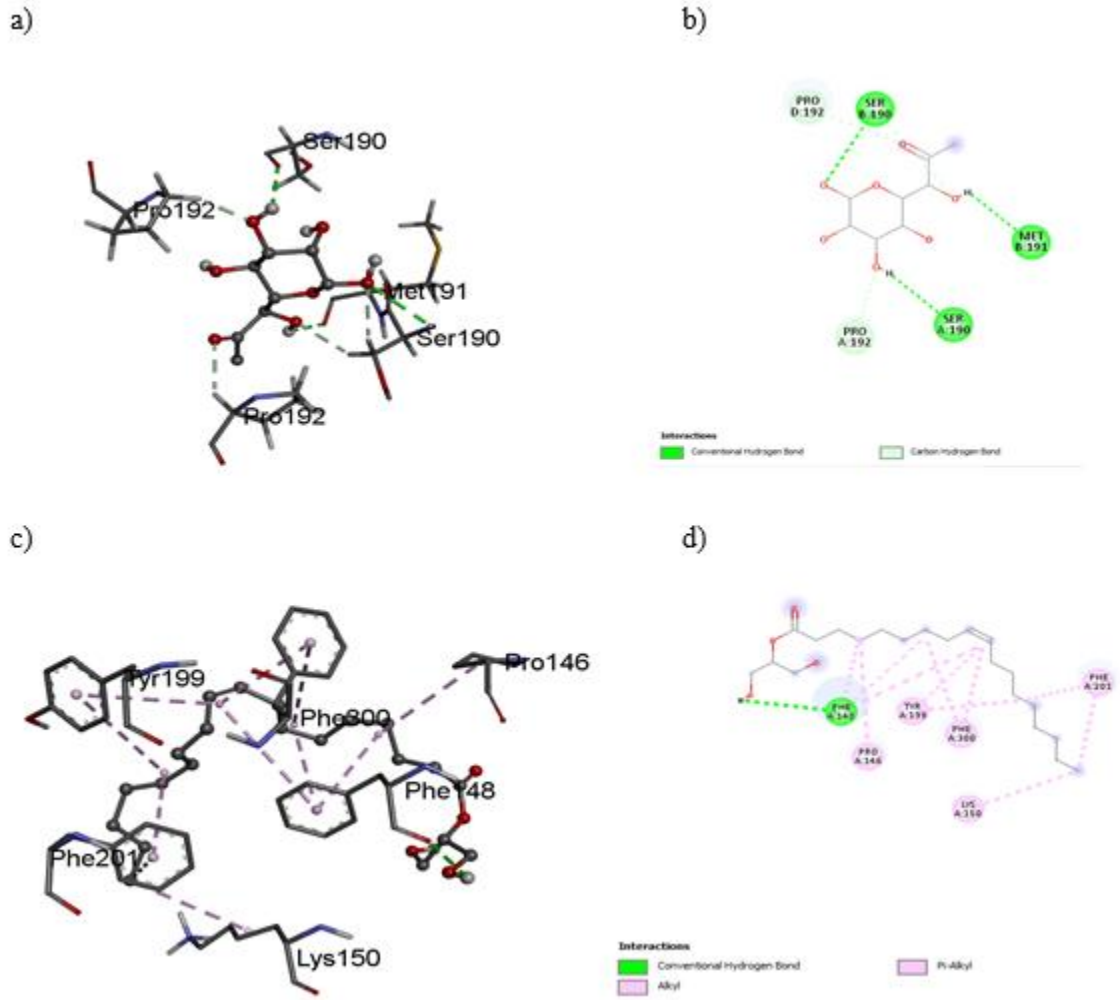

Figure 4(a-d): Representation of the molecular model of the compounds formed between compounds A, B, C, D and 1XU2, 2LV3, 6KMB

The interactive analyses are displayed in Figures 4(a-d). The obtained data showed that all compounds were well accommodated within the active site of the proteins. In the 3D interactions, the docked compounds are represented by cyan stick models, while the binding active residues are represented by grey stick models. The hydrogen bond interactions (HB) are depicted by the green dotted lines while alkyl and π-stacking interactions are shown by purple lines. In 2D, the docked compounds are represented by a grey stick color, while active binding sites are represented by three-letter codes. The HB interactions are shown by green and light blue dotted lines while the alkyl and π-stacking interactions are shown by purple lines.

Science World Journal Vol. 19(No 2) 2024 https://dx.doi.org/10.4314/swj.v19i2.15
www.scienceworldjournal.org
ISSN: 1597-6343 (Online), ISSN: 2756-391X (Print)
Published by Faculty of Science, Kaduna State University

ADMET protein-ligand molecular interaction predictions

Table 3: Docked complex (protein-ligand) molecular interactions

Entry	Hydrogen bond interactions	Carbon hydrogen bond interactions	Hydrophobic and other interactions
A(1XU2)	SER 190, MET 191	PRO 192, SER 190	---
B (1XU2)	SER 190, ASN 200	SER 190, PRO 192, ASN 200	PRO 192
C(1XU2)	GLN 7, CYS 8	GLU 12	PRO 34, TYR 13
D(1XU2)	ASN 200	SER 190	PRO 192
A(2LV3)	ARG 39, VAL 40, VAL 64, ASN 66, ASN 38	-----	-----
B (2LV3)	----	----	ARG 30, VAL 73, LEU 34, LEU 68, LEU 27
C (2LV3)	ASP 33	LEU 34	LEU 31, LEU 68, VAL 73, LEU 27, ARG 30, VAL 79, LEU 34
D(2LV3)	----	----	ARG 30, LEU 31, LEU 34, LEU 68, VAL 27, LEU 73
A (6KMB)	THR 211, THR 213, ASP 282, ARG 285, THR 209	----	ARG 285
B (6KMB)	PHE 148	----	TYR 199, PHE 300, PRO 146, LYS 150, PHE 201, PHE 148
C (6KMB)	SER 256	----	PHE 300, PHE 148, TYR 199
D (6KMB)	----	----	PHE 148, TYR 199, PHE 201, PHE 300

KEY: **A)** - 6-Acetyl-.beta.-d-mannose,
B) - 9-Octadecenoic acid (Z)-,2-hydroxy-1-(hydroxymethyl) ethyl ester
C) - 9-Octadecenoic acid (Z)-,2,3-dihydroxy propyl ester
D) - Z-4-Nonadecen-1-ol acetate

The Total Binding Energy for each protein with 4 ligands

From Table 3, the docking simulation of 4 ligands was performed for TNFR protein as displayed in Figure 4 and table 2. From the docking study, it was observed that compound A showed the best binding energy with the target TNFR protein with the value of -6.4 kcal/mol. Interaction analysis of the binding mode of compound A in the target protein reveals that a convectional hydrogen bond interaction was formed with SER 190 and MET 191 and also formed a carbon-hydrogen bond with PRO 192 and SER 190 and for GSH reductase protein as illustrated in table 2 it was observed that compound A showed the best binding affinity with the target protein having a binding energy value of -4.8 kcal/mol and showed a network of interactions. It formed a convectional hydrogen bond interaction with ARG 39, VAL 40, VAL 64, ASN 66, and ASN 38 and formed no carbon-hydrogen bond and other interactions as shown in table 3. For the TNFα protein, it was observed that compound B showed the best binding energy with the target TNFα protein with the value of -5.4 kcal/mol and interaction analysis of compound B in TNFα protein reveals that a convectional hydrogen bond interaction was formed with PHE 148 and formed no carbon-hydrogen bond but other interactions with PHE 300, PRO 146, LYS 150, PHE 201, TYR 199 and PHE 148 as depicted in table 3.

Science World Journal Vol. 19(No 2) 2024 https://dx.doi.org/10.4314/swj.v19i2.15
www.scienceworldjournal.org
ISSN: 1597-6343 (Online), ISSN: 2756-391X (Print)
Published by Faculty of Science, Kaduna State University

Druglikeness Properties

Table 4: Drug-likeness properties of the ligand molecules

COMPOUNDS	M.F	M.W (g/mol)	WlogP	H. bond acceptors	H. bond donors
		<500	<5	≤ 10	≤ 5
D	$C_{21}H_{40}O_2$	324.54	6.98	2	0
B	$C_{21}H_{40}O_4$	356.54	4.92	4	2
A	$C_8H_{14}O_7$	222.19	-3.26	7	5
C	$C_{21}H_{40}O_4$	356.54	4.92	4	2

KEY: M.F = Molecular Formula, M.W = Molecular weight, H. bond = Hydrogen bond
6-Acetyl-.beta.-d-mannose, **B)** 9-Octadecenoic acid (Z)-,2-hydroxy-1-(hydroxymethyl) ethyl ester, **C)** 9-Octadecenoic acid (Z)-,2,3-dihydroxy propyl ester, **D)** Z-4-Nonadecen-1-ol acetate

For a compound to be considered a good drug candidate, its physicochemical properties must determine great chances of bioavailability. In this study, Lipinski's rule of five was used to evaluate the drug-likeness of all molecules, as this parameter determines the physicochemical and drug-like properties of a compound (Table 4 and 5) Lipinski's rule of five states that if any small molecule violates more than two of these criteria (Molecular weight ≤ 500 g/mol, Number of hydrogen bond donors ≤ 5, Number of hydrogen bond acceptors ≤ 10, calculated logP ≤ 5), the molecule is said to be impermeable or badly absorbed (Lipinski *et al.,* 2004). Their Molecular Weight was < 500, and the number of hydrogen bond donors and acceptors for all were less than and equal to 5 and 10, respectively as illustrated in Table 4. The ADME results showed that compound D (Z-4-Nonadecen-1-ol acetate) only violated one rule from Lipinski's rule of five (WLOGP was > 5) while all others do not violate this rule, making them all an excellent oral drug. However, from the bioavailability radar which enables a first glance at the drug-likeness of a molecule and the region painted pink area which indicates the optimal range for each property (lipophilicity: XLOGP3 between − 0.7 and + 5.0, size: MW between 150 and 500 g/mol, polarity: TPSA between 20 and 130 A^2, solubility: log *S* not higher than 6, saturation: fraction of carbons in the sp3 hybridization not less than 0.25, and flexibility: no more than 9 rotatable bonds, it was observed that compounds A, B and D are not orally bioavailable due to high flexibility and lipophilicity, while compound C properties all fall within the optimal range, hence orally bioavailable. The toxicity of a drug is due to its high lipophilicity, leading to low absorption and solubility (Gao *et al.,* 2017).

Science World Journal Vol. 19(No 2) 2024 https://dx.doi.org/10.4314/swj.v19i2.15
www.scienceworldjournal.org
ISSN: 1597-6343 (Online), ISSN: 2756-391X (Print)
Published by Faculty of Science, Kaduna State University

The ADMET/ Pharmacokinetics Properties

The ADMET/Pharmacokinetics properties predicted for the five selected compounds are presented in Tables 5a, and 5b.

Table 5a: This table demonstrates the drug-likeness properties of the ligand molecules

ID	VALUE (LIGAND)			
	A	B	C	D
BBB	0.101259	7.51542	7.52996	16.073
Buffer_solubility_mg_L	295375	8.24582	20.3626	3.89077
$CaCO_3$	2.60739	35.4995	35.5023	57.1966
CYP_2C19_inhibition	Non	Inhibitor	Inhibitor	Inhibitor
CYP_2C9_inhibition	Inhibitor	Inhibitor	Inhibitor	Inhibitor
CYP_2D6_inhibition	Non	Non	Non	Non
CYP_2D6_subtrate	Non	Non	Non	Non
CYP_3A4_inhibition	Non	Inhibitor	Inhibitor	Inhibitor
CYP_3A4_subtrate	Weakly	Weakly	Weakly	Non
HIA	17.264955	92.568775	92.566355	100
MDCK	0.596461	72.4926	72.3689	69.126
Pgp_inhibition	Non	Non	Inhibitor	Inhibitor
Plasma_Protein_Binding	3.556372	100	100	100
Pure_water_solubility_mg_L	621031	2.05397	1.5698	0.12599
Skin_Permeability	-5.41637	-0.629347	-0.609651	-0.521987
SKlogD_value	-277315	6.06114	5.9715	7.85288
SKlogP_value	-277315	6.06114	5.9715	7.85288
SKlogS_buffer	0.123640	-4.63588	4.24328	-4.92124
SKlogS_pure	0.446380	-5.23952	5.35627	-6.41094

From Table 5a, compounds A, B, C, and D all exhibited poor skin permeability properties, but high plasma protein binding capability with a score of 100 except compound A having a score of 3.556372.

Table 5b: This table demonstrates the toxicity parameters of the ligand molecules retrieved from the pre-ADMET webserver

ID	VALUE (LIGAND)			
	A	B	C	D
algae_at	0.305686	0.0024585	0.00244603	0.00154819
Ames_test	mutagen	non-mutagen	non-mutagen	non-mutagen
Carcino_Mouse	negative	Positive	Negative	Negative
Carcino_Rat	positive	Negative	Negative	Negative
daphnia_at	42.663	0.00967801	0.0104895	0.0031907
hERG_inhibition	low_risk	low_risk	low_risk	low_risk
medaka_at	1578.04	0.000158509	0.000184385	1.74328e-005
minnow_at	482.721	0.000117387	0.000117444	7.42435e-006
TA100_10RLI	negative	Negative	Negative	Negative
TA100_NA	negative	Negative	Negative	Negative
TA1535_10RLI	positive	Negative	negative	Negative
TA1535_NA	negative	Negative	negative	Negative

As illustrated in Table 5b, the toxicity properties retrieved from the pre-ADMET webserver, compounds C and D showed low toxicity indications while compounds A and B showed carcinogenicity in Rats and mice.

Science World Journal Vol. 19(No 2) 2024 https://dx.doi.org/10.4314/swj.v19i2.15
www.scienceworldjournal.org
ISSN: 1597-6343 (Online), ISSN: 2756-391X (Print)
Published by Faculty of Science, Kaduna State University

Boiled-EGG analysis

The Boiled- egg plot between WLOGP and TPSA to predict gastrointestinal absorption and brain penetration of the selected molecules is shown below:

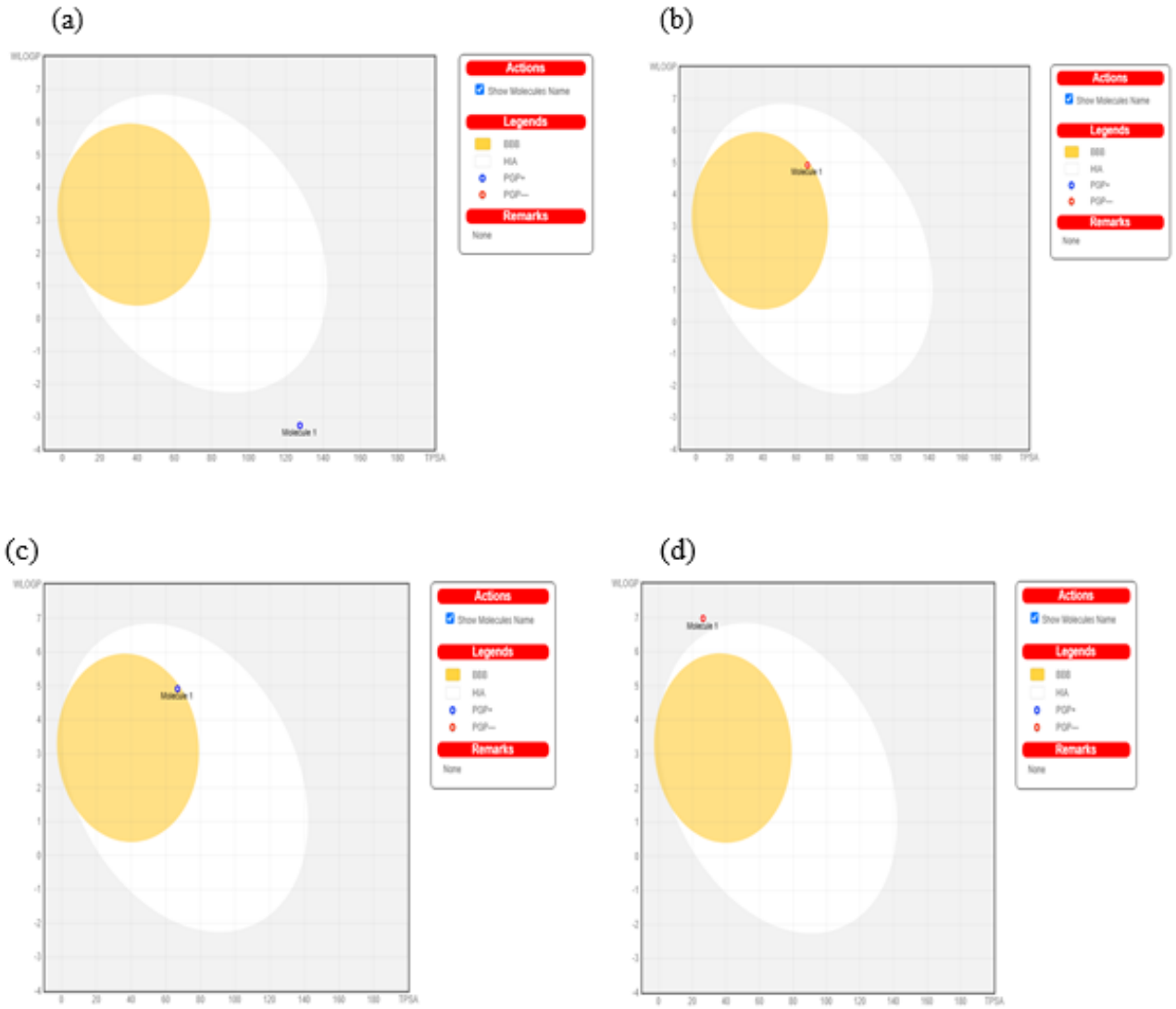

Fig. 5(a-d): The boiled egg plot SwissADME pharmacokinetics of the molecules

The pharmacokinetics of the molecules was investigated through SwissADME. The absorption of the molecules into the Blood–Brain Barrier (BBB) and Human Intestine Absorption (HIA) was demonstrated by the BOILED-Egg model. The BOILED-Egg allows for the intuitive evaluation of passive gastrointestinal absorption (HIA) and brain penetration (BBB) in the function of the position of the molecules in the WLOGP-*versus*-TPSA referential. The BBB and HIA are the common areas of absorption for a drug to be able to perform its function in the body. The yellow or the yolk represents the Blood-Brain Barrier while the white area represents human gastrointestinal absorption (HIA). The white part is the physicochemical space of molecules with the highest probability of being absorbed by the gastrointestinal tract, and the yellow part (yolk) is the physicochemical space of molecules with the highest probability of brain penetration. The model also evaluates a drug according to its properties to be a substrate or inhibitor of Pgp. This membrane protein is responsible for managing the efflux of substances in cells. The bioavailability and retention time of a drug is affected by its decreased permeability as it is more extruded in the intestine and BBB, leading to drug resistance (Janeea *et al.,* 2022). The points colored in blue are actively effluxed by P-gp (PGP+) and red for non-substrate of P-gp (PGP−). Compound A is not absorbed and not brain penetrant (outside the Egg) PGP+ (blue dot), Compound B and C are passively crossing the BBB (in the yolk), but compound C is pumped out from the brain (blue dot) (PGP+), while compound B is not subject to active efflux (red dot) (PGP−) and Compound D is not absorbed and not brain penetrant (outside the Egg) PGP- (red dot) Figure 5 (a, b, c and d).

Conclusion

In this study, it can be concluded that the esterification reaction for fatty acids and esters can be achieved using MOF catalyst

supported with silica (a heterogeneous catalyst that was synthesized by mechanochemical method- Cu-BDC@SiO_2) and ethanol as a reagent. The pretreatment using dilute sulfuric acid (acid hydrolysis) was efficient in the separating process of cell wall components resulting in hemicellulose hydrolysate. The second step for obtaining the sugars was carried out for the delignification stage because pretreatment conditions play a significant role in the amount of sugars released during the pretreatment step. Four compounds were formed from the esterification of fatty acids dehydrated from reducing sugars extracted from sugarcane bagasse. Identified compounds contribute beneficial role to human beings and are considered a new potential source of natural hepatoprotective use in many remedies.

For docking analysis for ligands, energy minimization was essential to determine the proper molecular arrangement in space since the drawn chemical structures are not energetically favorable. This was done to produce minimum interatomic energy values and form a more stable and optimal molecular conformation being stored in PDB format. The binding energy exhibits the extent of binding of the ligand molecule. The molecular docking explored the binding affinity of the four compounds from the esterification reaction with three target proteins of hepatoprotective. After a comparison of binding energy and amino acid residues, it was deduced that all four compounds have different hydrogen bonding, hydrophobic interactions, and different binding energies. Compounds A and B have the best binding energy compared to other compounds Furthermore, the best type of configuration would be the one that would bind with its target. To be effective as a drug, a potent molecule must reach its target in the body in sufficient concentration, and stay there in a bioactive form long enough for the expected biologic events to occur. Since none of the molecules violated more than one of Lipinski's rules of five, in this regard, the compounds showed good drug-likeness and pharmacokinetic scores, suggesting their potential to be highly bioavailable and active oral drugs. The molecules must show high biological activity together with low toxicity. The interactions of these bioactive compounds with the target proteins seem to be important factors in providing liver protection and might contribute to valorizing the potentialities of this plant against liver diseases. This indicated potential for the hepatoprotective activity of the esterified fatty acid esters against hepatoprotective receptors. Furthermore, the ADME analysis showed good gastric retention as well as good plasma protein binding proteins with very few predicted toxicity parameters. Based on the results, it can be concluded that the ligand molecules can be used for hepatoprotective.

Acknowledgments
The authors would like to thank the Department of Chemistry, Faculty of Pure and Applied Science, Umaru Musa Yaradua, University, Katsina for the provision of laboratory facilities.

REFERENCES

Adewusi, E. A., and Afolayan, A. J. (2010). A review of natural products with hepatoprotective activity. *Journal of Medicinal Plants Research*, 4 (13), 1318-1334. DOI:10.5897/JMPR09.472

Ariffin, K. K., Masngut, N., Seman, M. N. A. Jamek, S., and Sueb, M. S. M. (2020). Dilute acid hydrolysis pretreatment for sugar and organic acid production from pineapple residues. IOP. Conf. Series: *Materials Science and Engineering*, 991. 7 DOI: 10.1088/1757-899x/991/1/012057

Awoyale, A. A., and Lokhat, D. (2021). Experimental determination of the effects of pretreatments on selected Nigerian Lignocellulosic biomass in bioethanol production. *Sci. Rep*. 11, 557. https://doi.org/10.1038/s41598-020-78105-8

Bagheri, A. R., and Ghaedi, M. (2020). Application of Cu-based metal-organic framework (Cu-BDC) as a sorbent for dispersive solid phase extraction of gallic acid from orange juice sample using HPLC-UV method. *Arabian Journal of Chemistry*, 13; 5218-5228. https://doi.org/10.1016/j.arabjc.2020.02.020.

Chaparro, J., and Urbina, J-M. (2022). Methanol-Based Esterification of Palm Oil Sludge- Preparation of Palmitic and Oleic fatty acid Ethyl esters via Ethyl acetate transesterification. *Chemical Engineering Transactions*, 93:2283-9216. DOI:103303/CET2293059

Diana, A., and Zoete, V. (2016). A BOILED-Egg to predict gastrointestinal adsorption and brain penetration of small molecules. *ChemMedChem*., 11(11), 1117-1121. DOI: 10.1002/cmdc.201600182

Ezeonuegbu, B. A., Machido, D. A., Whong, C. M. Z., Japhet, W. S., Alexiou, A. Elazab, S. T., Qusty, N., Yaro, C. A., and Batiha, G. El-S. (2021). Agricultural waste of sugarcane bagasse as an efficient adsorbent for lead and nickel removal from untreated wastewater: Biosorption, equilibrium isotherms, kinetics, and desorption studies. *Biotechnology Reports*, 30. https://doi.org/10.1016/j.btre.2021.e00614.

Gao, Y., Gesenburg, C., and Zheng, W. (2017). Oral Formulations for Preclinical Studies: Principle, Design and Development Considerations. *Developing Solid Oral Dosage Forms*, AP, 2, 455-495

Guilherme, A. de A., Dantas, P. V. F., Soares, J. C. J., dos Santos, E. S., Fernandes, F. A. N., and de Macedo, G. R. (2017). Pretreatments and enzymatic hydrolysis of sugarcane bagasse aiming at the enhancement of the yield of glucose and xylose. *Brazilian Journal of Chemical Engineering*, 34(4), 937-947. DOI: 10.1590/0104-6632.20170344s20160225

Guo, T., Qiu, M., and Qi, X. (2019). Selective Conversion of biomass-derived Levulinic acid to Ethyl Levulinate catalyzed by Metal-organic framework (MOF)-supported polyoxometalates. *Applied Catalysis A, General*, 572, 168-175. DOI: 10.1016/j.apcata.2019.01.004

Hassan, M., Bala, S. Z., Bashir, M., Waziri, P. M. Adam, R. M., Umar, M. A., and Kini, P. (2022). LC-MS and GC-MS Profiling of Different Fractions of *Ficus Platyphylla* stem bark Ethanolic extract. *J. Anal. Meth. Chem.*, 14. DOI: 101155/2022/6349332

Inakar, M. B., and Lele, S. S. (2012). Extraction and Characterization of Sugarcane Peel Wax. *International Scholarly Research Network Agronomy*, 6. DOI:105402/2012/340158

Janeea, M. D. D. C., Sophia, A. A. D., Rianne, C. V., Alexis, M. L., and Myla, R. S-B. (2022). Molecular Docking and *In Silico* Pharmacological Screening of Oleosin from Cocos Nucifera Complexed with Tamoxifen in Developing Potential Breast Chemotherapeutic Leads. Asian Pac. J. Cancer Prev. 23(7), 2421-2430. DOI: 10.31557/APJCP.2022.23.72421

Jung, D., Korner, P., and Kruse, A. (2021). Kinetic Study on the Impact of Acidity and Acid Concentration on the Formation of 5-hydroxymethylfurfural (HMF), Humins and Levulinic acid in the Hydrothermal conversion of fructose. *Biomass Conv.*

Bioref. 11, 1155-1170. DOI: 10.1007/s13399-019-00507-0

Lipinski, C. A. (2004). Lead- and drug-like Compounds. The rule-of-five revolution. Drug *Discovery Today: Technologies*, 1(4). DOI:10.1016/j.ddtec.2004.11.007

Meharie, B. G., Amare, G. G., and Belayneh, Y. M. (2020). Evaluation of Hepatoprotective Activity of the Crude Extract and Solvent Fractions of Clutia Abyssinia (Euphorbiaceae) Leaf Against CCl4-Induced Hepatotoxicity in Mice. *Journal of Experimental Pharmacology*, 12, 137–150.

Muhammad, A., Katsayal, B. S., Forcados, G. E., Malami,I., Abubakar, I. B., kandi, A. I., Idris, A. M., Yusuf. S., Musa, S. M., Monday, N., and Umar, Z. S. (2020). In silico predictions on the possible mechanism of action of selected bioactive compounds against breast cancer. *In Silico Pharmacology*, 8:4. https://doi.org/10.1007/s40203-020-00057-8.

Peedikakkal, A. M. P., and Aljundi, I. H. (2020). Mixed-Metal Cu-BTC Metal-Organic Frameworks as a Strong Adsorbent for Molecular Hydrogen at Low Temperatures. *ACS Omega*. DOI: 10.1021/acsomega.0c02810

Salama, S. R., El-Hakam, A. S., Samra, E. S., El-Dafrawy, M. S. and Ahmed, I. A. (2018). Adsorption, Equilibrium, and Kinetic studies in the removal of Methyl Orange dye from Aqueous solution by using Copper Metal-Organic Framework (Cu-BDC). *Int. J. Modern Chem*., 10(2), 195-207

Sengupta, S., Bhowmik, R., Acharjee, S., and Sen, S. (2021). In-silico Modeling of 1-3-[3-(substituted phenyl) Prop-2-Enoyl] Phenyl Thiourea against Anti-inflammatory Drug Targets. *BioSci. Biotech. Res. Asia*, vol. 18(2), 413-421. DOI: 10.13005/bbra/2928

Swiss ADME (2017): a free web tool to evaluate pharmacokinetics, drug-likeness, and medicinal chemistry friendliness of small molecules. *Sci. Rep*., 7, 42717

Taghizadeh, M. S., Niazi A., Moghadam, A., and Afsharifar, A. (2022). Experimental, molecular docking, and molecular dynamic studies of natural products targeting overexpressed receptors in breast cancer. *PLoS ONE* 17(5): e0267961. https://doi.org/10.1371/journal.pone.0267961